



Automatic Generation of Stochastically Dominant Modes of Structural Failure in Frame Structure

メタデータ	言語: eng 出版者: 公開日: 2010-04-06 キーワード (Ja): キーワード (En): 作成者: Murotsu, Yoshisada, Okada, Hiroo, Yonezawa, Masaaki, Martin, Grimmelt, Taguchi, Katashi メールアドレス: 所属:
URL	https://doi.org/10.24729/00008619

Automatic Generation of Stochastically Dominant Modes of Structural Failure in Frame Structure

Yoshisada MUROTSU*, Hiroo OKADA*, Masaaki YONEZAWA**,
Martin GRIMMELT *** and Katashi TAGUCHI*

(Received November 15, 1981)

This paper proposes a method to evaluate the upper bound for the structural failure probability of frame structures by automatically generating the failure modes and their safety margins and by systematically selecting the stochastically dominant modes of failure. The validity of the proposed method is demonstrated through numerical examples and the relationship of the proposed method to the conventional methods is discussed. It is shown that the proposed method is also applicable to the automatic generation of stochastically dominant modes and their mode equations needed for the conventional methods.

1. Introduction

Many studies have been made of methods of reliability analysis in structures,^{1) - 7)} where modes of failure are specified *a priori*. However, there are too many modes of structural failure in redundant structures to count all of them in practice.^{7) - 10)} The present authors^{11) - 15)} have proposed a method of automatically generating the failure modes of truss structures and evaluating reliability. For frame structures with rigid joints, some approaches have been initiated to automatically generate the failure modes¹⁶⁾ and to perform reliability assessment based on them.^{15), 17)} Nevertheless, there are no systematic methods available for reliability analysis of the frame structures by automatically generating the failure modes and their mode equations.

This paper is concerned with automatic generation of failure modes in frame structures and reliability assessment. First, structural failure is defined as formation of a mechanism in the structures, and a method is proposed for automatically generating failure modes and their safety margins by using a Matrix method. Second, an upper bound of the structural failure probability is evaluated by systematically selecting the stochastically dominant modes of structural failure through branching and bounding operations. Finally, numerical examples are presented to demonstrate the validity of the proposed method. Further, discussions are made of the relationship between the proposed method and the conventional methods where the failure modes and their mode equations need to be predetermined.

* Department of Naval Architecture.

** Department of Industrial Engineering, Kinki University, Kowakae, Higashi-Osaka.

*** Formerly, Visiting Research Associate at Department of Naval Architecture. Presently, Technische Universität München, Institut für Bauingenierwesen III, 8000 München 2, West Germany.

2. Automatic Generation of Failure Modes and Mode Equations

In frame structures, many types of failure criteria are applied to the members of the structures, depending on the configuration of the structures, shapes of the members, loading conditions, *etc.* We consider here a simple type of plane frame structures whose members are uniform and homogeneous and to which only concentrated forces and moments are applied. Members are assumed to fail when the applied bending moments reach their fully plastic moments and plastic hinges form in them. In the frame structures to be considered, critical sections where plastic hinges may form are the joints of the members and the places at which the concentrated forces are applied. Those potential plastic hinged sections are taken as the member ends to facilitate stress analysis, which means that unit members are the parts of the original members which are connected by the critical sections.

Consider a frame structure with n members and l loads applied to its nodes. Let the left- and right-hand ends of a member i ($i = 1, 2, \dots, n$) be serially numbered as $2i-1$ and $2i$, respectively. Here, the bending moments of the member ends are calculated by using a Matrix method and written in the form:

$$S_i = \sum_{j=1}^l b_{ij}(I) L_j \quad (i = 1, 2, \dots, 2n) \quad (1)$$

where L_j are the applied loads and I is a vector composed of the moments of inertia of area I_j of the members, *i.e.*, $I = (I_1, I_2, \dots, I_n)^T$.

The strengths of the member ends are given by the fully plastic moments of the members, *i.e.*,

$$R_{2i-1} = R_{2i} = AZ_{pi} C_{yi} \quad (i = 1, 2, \dots, n) \quad (2)$$

where AZ_{pi} is plastic section modulus of the i -th member and C_{yi} yield stress.

The safety margins of the member ends are

$$Z_i = R_i - S_i \quad (i = 1, 2, \dots, 2n) \quad (3)$$

Consequently, the failure criterion of the member end is given by

$$Z_i \leq 0 \quad (4)$$

When a member end is turned into a plastic hinge, it is treated as in the following¹⁸⁾, which enables us to perform stress analysis with the number of the nodes unchanged.

When a plastic hinge forms at the left-hand end $2i-1$ of a member i shown in Fig. 1 (b), the original stiffness matrix of the member:

$$[k_i] = \begin{bmatrix} EA/l & 0 & 0 & -EA/l & 0 & 0 \\ & 12EI/l^3 & 6EI/l^2 & 0 & -12EI/l^3 & 6EI/l^2 \\ & & 4EI/l & 0 & -6EI/l^2 & 2EI/l \\ & & & EA/l & 0 & 0 \\ \text{SYM.} & & & & 12EI/l^3 & -6EI/l^2 \\ & & & & & 4EI/l \end{bmatrix} \quad (5)$$

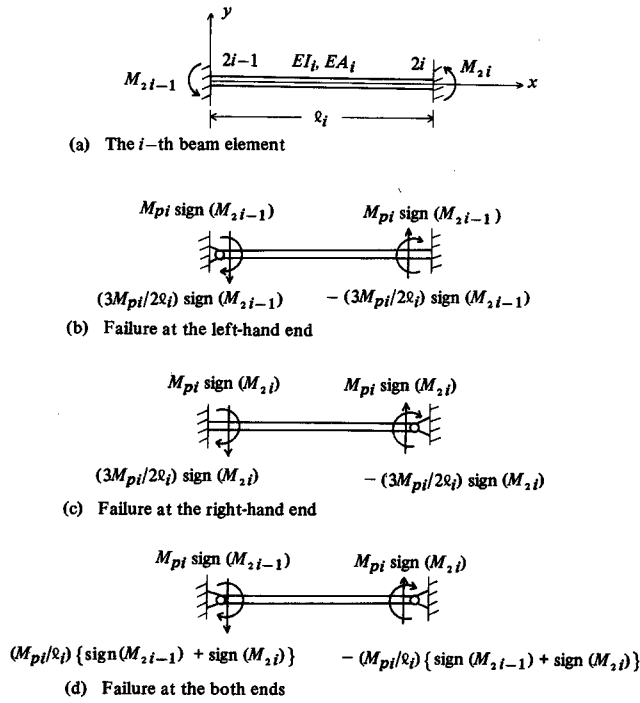


Fig. 1 Beam element and treatment of plastic hinged ends ($M_{pi} = AZ_{pi} C_{yi}$)

is replaced by a reduced matrix :

$$[k_i^L] = \begin{bmatrix} EA/L & 0 & 0 & -EA/L & 0 & 0 \\ 3EI/l^3 & 0 & 0 & 0 & -3EI/l^3 & 3EI/l^2 \\ & & 0 & 0 & 0 & 0 \\ & & & EA/l & 0 & 0 \\ \text{SYM.} & & & & 3EI/l^3 & -3EI/l^2 \\ & & & & & 3EI/l \end{bmatrix} \quad (6)$$

and artificial forces and moments are applied to the ends as indicated in Fig. 1 (b).

Similarly, when the right-hand end $2i$ is turned into a plastic hinge, the member stiffness matrix is taken as

$$[k_i^R] = \begin{bmatrix} EA/l & 0 & 0 & -EA/l & 0 & 0 \\ 3EI/l^3 & 3EI/l^2 & 0 & 0 & -3EI/l^3 & 0 \\ & 3EI/l & 0 & 0 & -3EI/l^2 & 0 \\ & & EA/l & 0 & 0 & 0 \\ \text{SYM.} & & & 3EI/l^3 & 0 & 0 \\ & & & & 0 & 0 \end{bmatrix} \quad (7)$$

and artificial nodal forces are given as shown in Fig. 1 (c).

Finally, when both ends are transformed into plastic hinges, the reduced stiffness matrix of the member is

$$[k_i^{LR}] = \begin{bmatrix} EA/l & 0 & 0 & -EA/l & 0 & 0 \\ & 0 & 0 & 0 & 0 & 0 \\ & & 0 & 0 & 0 & 0 \\ & & & EA/l & 0 & 0 \\ \text{SYM.} & & & & 0 & 0 \\ & & & & & 0 \end{bmatrix} \quad (8)$$

and applied nodal forces are as illustrated in Fig. 1 (d).

In a statically indeterminate frame structure, failure in any one member end does not necessarily result in structural failure. Structural failure is defined as formation of a mechanism in the structure. A failure mode is generated as in the following manner. When any one member end fails, redistribution of the internal forces arises among the member ends in survival and a member end next to fail is determined. After repeating the similar processes, structural failure results when the member ends up to some specified number p_k , e.g., member ends r_1, r_2, \dots , and r_{p_k} , have failed. Formation of a mechanism is determined by investigating the singularity of the total structure stiffness matrix $[K^{(p_k)}]$ formed by using the reduced member stiffness matrices for the failed members, i.e., members with plastic hinges. Then, a criterion for structural failure is given by

$$|[K^{(p_k)}]| = 0 \quad (9)$$

where $|[.]|$: the determinant of a matrix $[.]$.

Now introduce the expressions of the safety margins for the member ends in survival after some member ends are in failure. For instance, when member ends r_1, r_2, \dots , and r_p have failed, their stiffness matrices are replaced by the reduced ones and their residual strengths are applied to the nodes as artificial nodal forces, as mentioned before. Then, stress analysis of the structure is carried out once again by using a Matrix method, and the internal forces of the surviving member ends are determined and written in the form:

$$\begin{aligned} S_{i(r_1, r_2, \dots, r_p)} &= \sum_{j=1}^l b_{ij}^{(p)} (I) L_j^{(p)} \\ &= \sum_{j=1}^l b_{ij}^{(p)} (I) L_j - a_{ir_1} R_{r_1} - a_{ir_2} R_{r_2} - \dots - a_{ir_p} R_{r_p} \end{aligned} \quad (10)$$

where suffix (r_1, r_2, \dots, r_p) denotes a set of the failed member ends arranged in the sequential order of failure. Consequently, the safety margins are given by

$$\begin{aligned} Z_{i(r_1, r_2, \dots, r_p)} &\triangleq R_i - S_{i(r_1, r_2, \dots, r_p)} \\ &= (R_i + a_{ir_1} R_{r_1} + a_{ir_2} R_{r_2} + \dots + a_{ir_p} R_{r_p}) \\ &\quad - \sum_{j=1}^l b_{ij}^{(p)} (I) L_j \end{aligned} \quad (11)$$

Structural failure of the redundant frame structure occurs when all of the p_k member

ends, e.g., r_1, r_2, \dots , and r_{p_k} , are subjected to failure. Hence, a criterion of structural failure is also expressed by using the safety margins of the failed member ends:

$$Z_{r_p}(r_1, r_2, \dots, r_{p-1}) \leq 0 \quad (p = 1, 2, \dots, p_k) \quad (12)$$

It should be noted here that the safety margin $Z_{r_{p_k}}(r_1, r_2, \dots, r_{p_k-1})$ of the last hinged member end r_{p_k} is identical to the failure mode equation derived by application of the principle of virtual work to the conventional failure mode^{1)~7)} resulting from failure of the member ends r_1, r_2, \dots , and r_{p_k} .

3. Selection of Stochastically Dominant Failure Modes and Reliability Evaluation

An algorithmic procedure is proposed which systematically evaluates an upper bound of the structural failure probability by selecting only the dominant modes of failure and evaluating the contribution of the others. That is, the upper bound is estimated by

$$P_{fU} = \sum_i P_{fi} + E \quad (13)$$

where P_{fi} 's are the upper bounds of failure probabilities of the selected dominant modes and E the contribution of the discarded modes. The procedure consists mainly of (i) branching operations, (ii) adjustment of the upper bound, and (iii) bounding operations, which will be briefly described.

The following notations are used for failure events. When a sequential failure of the member ends r_1, r_2, \dots , and r_{p_k} turns a structure into a mechanism, failure event of the member end r_p is denoted as

$$F_{r_p}^{(p)} = (Z_{r_p}(r_1, r_2, \dots, r_p) \leq 0) \quad (14)$$

From the failure criterion (12), the corresponding failure event of the structure is given by

$$W_{kq} = F_{r_1}^{(1)} \cap F_{r_2}^{(2)} \cap \dots \cap F_{r_{p_k}}^{(p_k)} = \bigcap_{p=1}^{p_k} F_{r_p}^{(p)} \quad (15)$$

The structural failure probability is expressed as

$$P_f = \text{Prob} \left[\bigcup_{k=1}^m \bigcup_{q=1}^{p_k!} W_{kq} \right] \quad (16)$$

where m is the number of combinations of the member ends to cause structural failure. Upper bounds are also estimated by^{11)~15)}

$$\begin{aligned} P_{fU}^{(1)} &= \sum_{i=1}^n \text{Prob} [F_i^{(1)}] \\ P_{fU}^{(2)} &= \sum_{k=1}^m \sum_{q=1}^{p_k!} \text{Prob} [W_{kq}] \end{aligned} \quad (17)$$

Branching operations. This is an operation which selects a combination of member ends to make the structure a mechanism so that the selected combination of member ends may yield a failure mode with a large failure probability. The member end with the largest value of failure probability is selected as the member end to fail at the first stage r_1 , i.e.

$$\text{Prob} [F_{r_1}^{(1)}] \triangleq \max_{i_1 \in I_{s1}} \text{Prob} [F_{i_1}^{(1)}]$$

where I_{s1} denotes a set of member ends left to be selected at the first stage. The member end to fail at the p -th stage r_p ($p > 1$) is determined so that the joint failure probability of the member end first to fail and the member end to be selected is maximized. That is,

$$\text{Prob} [F_{r_1}^{(1)} \cap F_{r_p}^{(p)}] \triangleq \max_{i_p \in I_{sp}} (\text{Prob} [F_{r_1}^{(1)} \cap F_{i_p}^{(p)}]) \quad (19)$$

where I_{sp} denotes a set of member ends left to be selected at the p -th stage.

The operations of selecting member ends to fail are continued until a combination of member ends is determined to make the structure a mechanism.

Adjustment of upper bound. When a combination of the member ends to cause structural failure is found, the probability of occurrence of the failure mode is approximated by

$$\begin{aligned} \text{Prob} \left[\bigcap_{p=1}^{pk} F_{r_p}^{(p)} \right] &\simeq \min [\text{Prob} [F_{r_1}^{(1)} \cap F_{r_2}^{(2)}], \text{Prob} [F_{r_1}^{(1)} \cap F_{r_3}^{(3)}], \\ &\dots, \text{Prob} [F_{r_1}^{(1)} \cap F_{r_{pk}}^{(pk)}]] \\ &\triangleq P_{fL}^* \end{aligned} \quad (20)$$

This value is added to the partial sum of the probabilities P_{fU}^* , i.e., $P_{fU}^* = P_{fU}^* + P_{fL}^*$. By comparing P_{fL}^* thus calculated with the maximum value so far obtained P_{fL} , P_{fL} is replaced by P_{fL}^* if $P_{fL}^* > P_{fL}$.

Bounding operations. This is an operation to select the member ends to be discarded. That is, the member ends to be eliminated from a set of the member ends to be selected at the p -th stage are determined by the following criteria:

(a) in case of $p = 1$;

$$\text{Prob} [F_{i_1}^{(1)}] / P_{fL} < 10^{-\eta} \text{ for } i_1 \in I_{s1} \quad (21)$$

(b) in case of $p > 1$;

$$\text{Prob} [F_{r_1}^{(1)} \cap F_{i_p}^{(p)}] / P_{fL} < 10^{-\eta} \text{ for } i_p \in I_{sp} \quad (22)$$

where η is a constant^{(11), (12)}. The maximum contribution of the discarded member ends to the upper bound is evaluated by

$$\left. \begin{array}{l} \text{Prob} [F_{i_1}^{(1)}] \text{ for } p = 1 \\ \text{Prob} [F_{r_1}^{(1)} \cap F_{i_p}^{(p)}] \text{ for } p \geq 2 \end{array} \right\} \quad (23)$$

Consequently, these are added to the partial sum P_{fU}^* . Finally, P_{fU}^* gives the upper bound P_{fU}^* to be estimated. There is another bounding criterion adopted in the proposed algorithmic procedure which assures computation efficiency^{11), 12)}. These bounding operations are repeated until no member ends are left to be selected.

4. Numerical Examples

Numerical examples are presented to discuss the properties of the proposed method for reliability analysis of redundant frame structures. Applied loads and strengths of structural members are assumed to be Gaussian random variables. The loads and strengths are statistically independent while the correlation between the loads is taken into account.

4.1 Portal frame with vertical load

Consider a portal frame with a vertical load applied as shown in Fig. 2 (a). Data concerned are given in Table 1 (a). For the structure, there exist twenty four modes of structural failure which are classified into four final forms of structural failure illustrated in Fig. 2 (b). The various upper bounds of structural failure probability are evaluated and listed in Table 1 (b). The upper bound P_{fU} calculated by the proposed method is smaller than $P_{fU}^{(1)}$, i.e., the bound evaluated as a sum of the failure probabilities of all the member ends. It is also seen that P_{fU} gives almost the same values as $P_{fU}^{(2)}$, i.e., a sum of the failure probabilities of all the structural failure modes.

In the conventional methods of reliability analysis,¹⁾⁻⁷⁾ the final forms of structural failure are first assumed as shown in Fig. 2 (b), and their safety margins are derived by applying the principle of virtual work as follows;

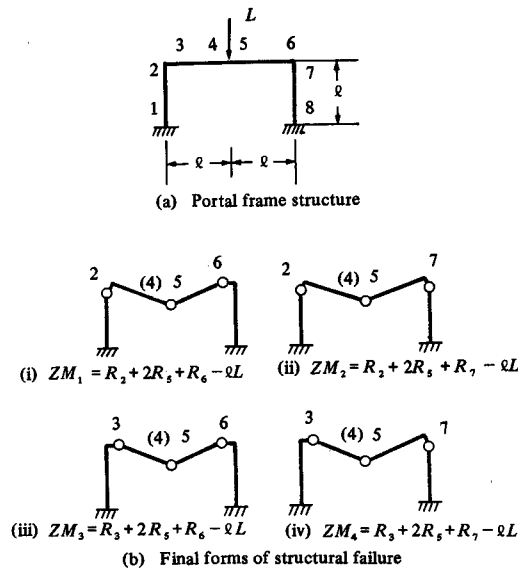


Fig. 2 Portal frame structure and final forms of structural failure

Table 1 Reliability assessment of portal frame with vertical load

(a) Data of portal frame

Member end number	Plastic section modulus AZ_{pi} m ³	Mean value of yield stress $\bar{\sigma}_{Yi}$ MPa
1, 2	0.489×10^{-3}	276
3, 4	0.367×10^{-3}	276
5, 6	0.367×10^{-3}	276
7, 8	0.489×10^{-3}	276

$$\bar{L} = 40 \text{ kN}, \quad l = 5 \text{ m}$$

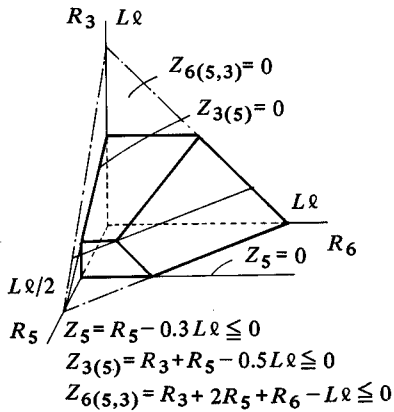
(b) Upper bounds of structural failure probability ($\eta = 3.0$)

$CV_{\sigma_{Yi}}$	CV_{L_j}	P_{fU}	$P_{fU}^{(1)}$	$P_{fU}^{(2)}$	$\Sigma P [ZM_i \leq 0]$
0.1	0.3	0.2100×10^{-2}	0.2317×10^{-1}	0.2099×10^{-2}	0.1101×10^{-2}
0.05	0.3	0.9925×10^{-3}	0.1383×10^{-1}	0.9924×10^{-3}	0.5259×10^{-3}
0.1	0.15	0.1495×10^{-6}	0.1180×10^{-2}	0.1494×10^{-6}	0.7417×10^{-7}
0.05	0.15	0.1025×10^{-8}	0.3329×10^{-4}	0.1025×10^{-8}	0.1430×10^{-9}

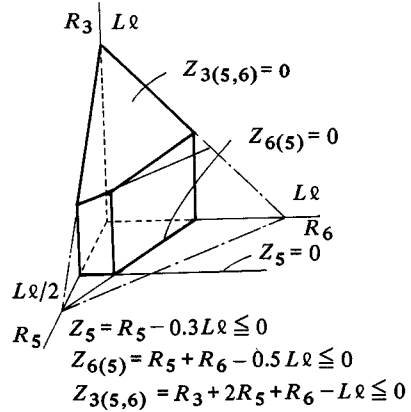
$$\begin{aligned} ZM_1 &= R_2 + 2R_5 + R_6 - lL \\ ZM_2 &= R_2 + 2R_5 + R_7 - lL \\ ZM_3 &= R_3 + 2R_5 + R_6 - lL \\ ZM_4 &= R_3 + 2R_5 + R_7 - lL \end{aligned} \quad (24)$$

As noted in section 2, these safety margins are the same as those of the last hinged member ends to form a mechanism. The upper bounds $\sum_{i=1}^4 P [ZM_i \leq 0]$'s, calculated by using equations (24) are also given in Table 1 (b). It is seen that the proposed upper bounds P_{fU} 's are very different from those upper bounds. These discrepancies are caused by the following reasons. Corresponding to the final forms of the structural failure mode (iii) in Fig. 2 (b), there are six modes of structural failure when the sequential order of failure is taken into account. Those failure modes are 5 \rightarrow 3 \rightarrow 6 (this means that the sequential order of failure of member ends is 5, 3 and 6), 5 \rightarrow 6 \rightarrow 3, 3 \rightarrow 5 \rightarrow 6, 3 \rightarrow 6 \rightarrow 5, 6 \rightarrow 5 \rightarrow 3 and 6 \rightarrow 3 \rightarrow 5.

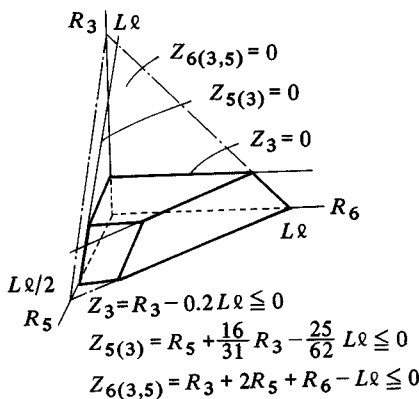
The failure regions of those modes are depicted in Figs. 3 (a) to (f), which are determined by the criterion, equation (12), using the safety margins of the member ends at the respective failure stages. On the other hand, the failure region given by $ZM_3 \leq 0$ is a sum of the six failure regions in Fig. 3. Consequently, when the failure probabilities of those failure modes are summed up to evaluate the upper bound, the resulting bound yields a larger value than the bound calculated by using equation (24). The reason for this is that the failure probabilities of the events corresponding to the intersecting regions are added multiple times. Another reason for the proposed bound to be larger is due to the fact that



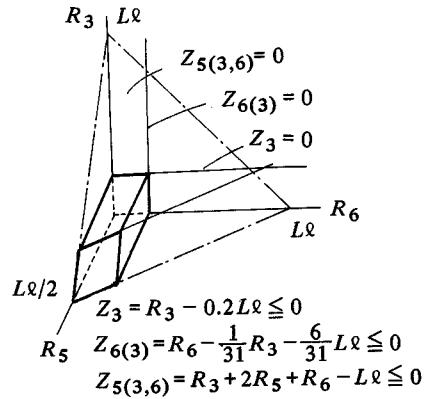
(a) Order of failure 5 → 3 → 6



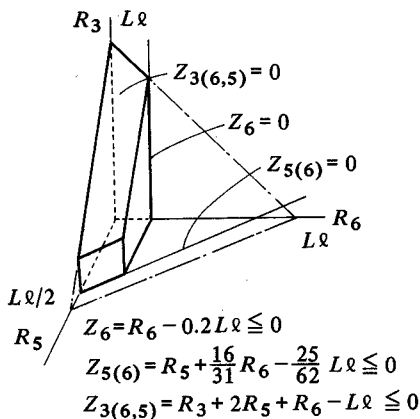
(b) Order of failure 5 → 6 → 3



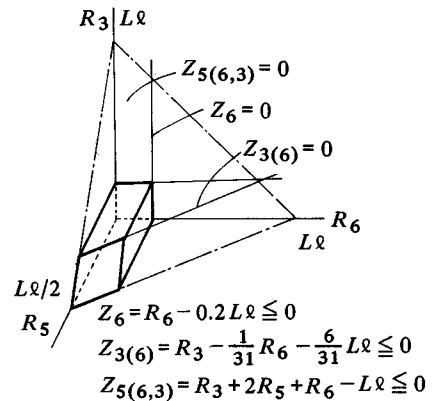
(c) Order of failure 3 → 5 → 6



(d) Order of failure 3 → 6 → 5

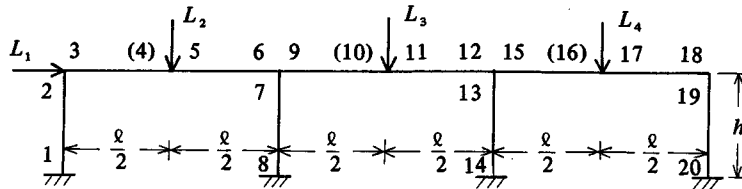


(e) Order of failure 6 → 5 → 3

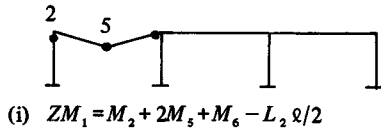


(f) Order of failure 6 → 3 → 5

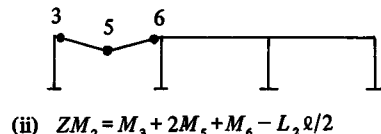
Fig. 3 Failure regions of structural failure modes



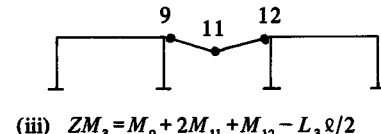
(a) Three span portal frame



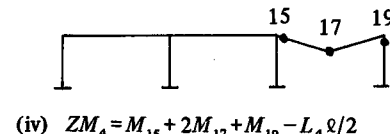
(i) $ZM_1 = M_2 + 2M_5 + M_6 - L_2 \varrho/2$



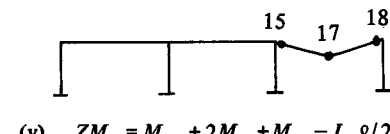
(ii) $ZM_2 = M_3 + 2M_5 + M_6 - L_2 \varrho/2$



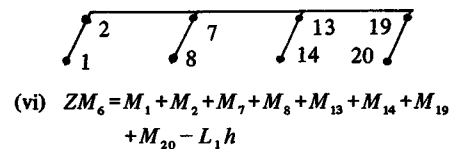
(iii) $ZM_3 = M_9 + 2M_{11} + M_{12} - L_3 \varrho/2$



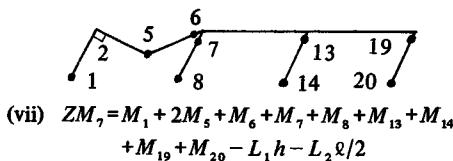
(iv) $ZM_4 = M_{15} + 2M_{17} + M_{19} - L_4 \varrho/2$



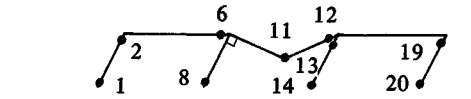
(v) $ZM_5 = M_{15} + 2M_{17} + M_{19} - L_4 \varrho/2$



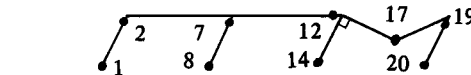
(vi) $ZM_6 = M_1 + M_2 + M_7 + M_8 + M_{13} + M_{14} + M_{19} + M_{20} - L_1 h$



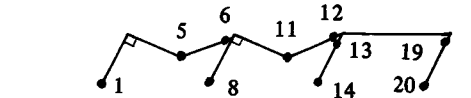
(vii) $ZM_7 = M_1 + 2M_5 + M_6 + M_7 + M_8 + M_{13} + M_{14} + M_{19} + M_{20} - L_1 h - L_2 \varrho/2$



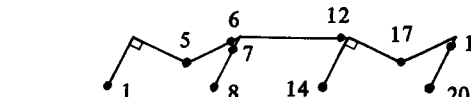
(viii) $ZM_8 = M_1 + M_2 + M_6 + M_8 + 2M_{11} + M_{12} + M_{13} + M_{14} + M_{19} + M_{20} - L_1 h - L_3 \varrho/2$



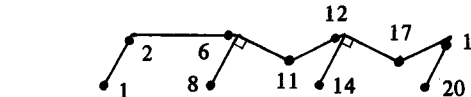
(ix) $ZM_9 = M_1 + M_2 + M_7 + M_8 + M_{12} + M_{14} + 2M_{17} + 2M_{19} + M_{20} - L_1 h - L_4 \varrho/2$



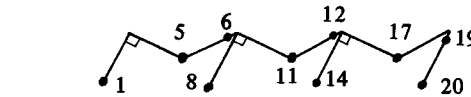
(x) $ZM_{10} = M_1 + 2M_5 + M_6 + M_8 + 2M_{11} + M_{12} + M_{13} + M_{14} + M_{19} + M_{20} - L_1 h - (L_2 + L_3) \varrho/2$



(xi) $ZM_{11} = M_1 + 2M_5 + M_6 + M_7 + M_8 + M_{12} + M_{14} + 2M_{17} + 2M_{19} + M_{20} - L_1 h - (L_2 + L_4) \varrho/2$



(xii) $ZM_{12} = M_1 + M_2 + M_6 + M_8 + 2M_{11} + 2M_{12} + M_{14} + 2M_{17} + 2M_{19} + M_{20} - L_1 h - (L_3 + L_4) \varrho/2$



(xiii) $ZM_{13} = M_1 + 2M_5 + 2M_6 + M_8 + 2M_{11} + 2M_{12} + M_{14} + 2M_{17} + 2M_{19} + M_{20} - L_1 h - (L_2 + L_3 + L_4) \varrho/2$

(b) Final forms of structural failure

Fig. 4 Three span portal frame and examples of final forms of structural failure ($M_i = R_i$)

the three dimensional joint probabilities are approximated by the two dimensional marginal probability distribution functions, *i.e.*, equation (20).

4.2 Three span frame

Reliability assessment is made of three span frame shown in Fig. 4 (a). Data concerned are given in Table 2 (a). The calculated upper bounds are listed in Table 2 (b). Some of final forms of structural failure are given in Fig. 4 (b), for applying the conventional methods of reliability analysis. On the other hand, there are many types of structural failure modes selected in the proposed method. However, they are classified into two groups depending on the properties of the sets of failed member ends to form mechanisms, *i.e.*,

- (i) Sets of failed member ends, in which a mechanism is not formed if any one failed member end belonging to the sets is removed. These sets of failed member ends are called minimum sets of failed member ends.
- (ii) Sets of failed member ends, in which there are some redundant member ends to form a mechanism and thus the structure is turned into a mechanism even if these member ends are removed from the sets.

Table 2 Reliability assessment of three span portal frame

(a) Data of three span portal frame

Member end number	Plastic section modulus $AZ_{pi} \text{ m}^3$	Mean value of yield stress $\bar{\sigma}_{Yi} \text{ MPa}$
1, 2	0.272×10^{-3}	276
3, 4	0.367×10^{-3}	276
5, 6	0.367×10^{-3}	276
7, 8	0.272×10^{-3}	276
9, 10	0.367×10^{-3}	276
11, 12	0.367×10^{-3}	276
13, 14	0.272×10^{-3}	276
15, 16	0.367×10^{-3}	276
17, 18	0.367×10^{-3}	276
19, 20	0.272×10^{-3}	276

$$\bar{L}_1 = 50 \text{ kN}, \bar{L}_2 = \bar{L}_3 = \bar{L}_4 = 40 \text{ kN}, h = 5 \text{ m}, l = 10 \text{ m}$$

(b) Upper bounds ($\eta = 2.0$)

$CV_{\sigma_{Yi}}$	CV_{L_j}	P_{fU}	$P_{fU}^{(1)}$	$\Sigma P [ZM_i \leq 0]$
0.05	0.3	0.9314×10^{-1}	0.1420×10^0	0.4991×10^{-2}
0.1	0.3	0.1684×10^0	0.2405×10^0	0.8469×10^{-2}

Mean processing time by ACOS/NEAC 700 : 17 min/case

Examples of the minimum sets of failed member ends are the structural failure modes which are reduced to the final forms of structural failure shown in Fig. 4 (b). Structural failure modes belonging to the sets (ii) are transformed into the minimum sets (i) by removing the redundant member ends from the original sets. It should be noted here that the safety margins of the last hinged member ends are the same for all the structural failure modes belonging to the same minimum sets of failed member ends, which fact is proved

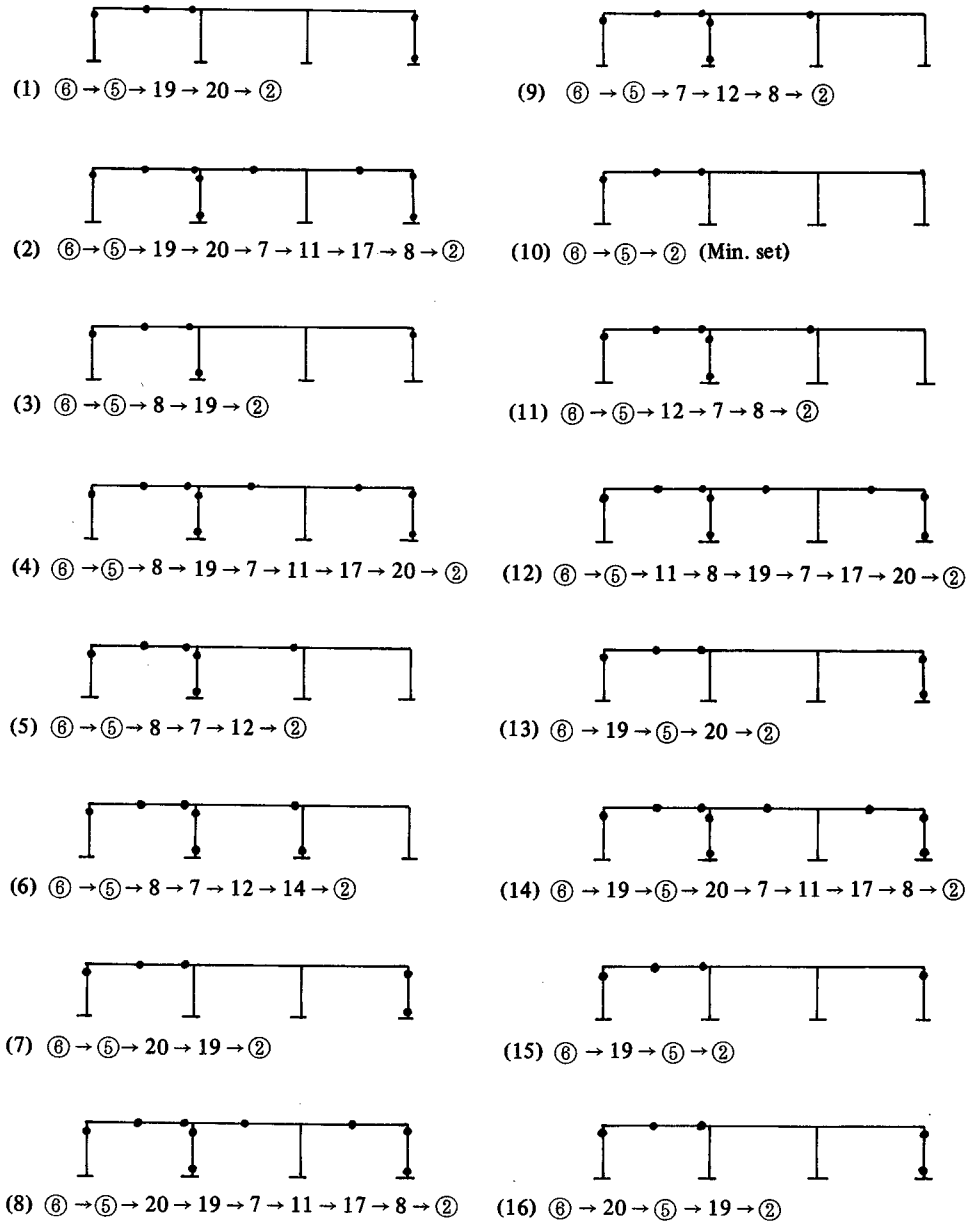


Fig. 5 Examples of structural failure modes with the same minimum set of the failed member ends { 2, 5, 6 }.

from the theorem on uniqueness of a plastic collapse mechanism. As noted in section 2, the safety margins derived by applying the principle of virtual work to these failure modes are also the same, and thus all of these modes are treated as one structural failure mode in the conventional methods. Fig. 5 shows some of the failure modes which are selected in the present method and reduced to the minimum sets of the failed member ends { 2, 5, 6 } corresponding to the final forms of structural failure in Fig. 4 (b) - (i). The minimum sets of failed member ends and the numbers of the selected modes which are reduced to these minimum sets are also listed in Table 3. It is seen that only six minimum sets of failed member ends are selected and a large number of failure modes selected are reduced to them.

Table 3 Selected minimum sets of failed member ends and numbers of selected structural failure modes reduced to these minimum sets.

($\eta = 2.0$)

No. of Min. set (See Fig. 4)	Load factor λ_i	$CV_{\sigma Y_i}/CV_{L_j} = 0.05/0.3$		$CV_{\sigma Y_i}/CV_{L_j} = 0.1/0.3$	
		Selected modes*	P [$ZM_i \leq 0$]	Selected modes*	P [$ZM_i \leq 0$]
(i)	1.89	493	0.1807×10^{-2}	395	0.2910×10^{-2}
(ii)	2.02	58	0.4342×10^{-3}	130	0.8353×10^{-3}
(iii)	2.02	53	0.4342×10^{-3}	70	0.8353×10^{-3}
(iv)	1.89	93	0.1807×10^{-2}	142	0.2910×10^{-2}
(v)	2.02	3	0.4342×10^{-3}	9	0.8353×10^{-3}
(vi)	2.40	0	0.1912×10^{-5}	0	0.3553×10^{-5}
(vii)	1.84	124	0.5050×10^{-4}	129	0.8636×10^{-4}
(viii)	2.06	0	0.4316×10^{-6}	0	0.1091×10^{-5}
(ix)	2.01	0	0.1665×10^{-5}	0	0.4020×10^{-5}
(x)	1.78	0	0.5262×10^{-5}	0	0.1266×10^{-4}
(xi)	1.74	0	0.1423×10^{-4}	0	0.2972×10^{-4}
(xii)	1.90	0	0.2211×10^{-6}	0	0.7653×10^{-6}
(xiii)	1.72	0	0.1491×10^{-5}	0	0.4597×10^{-5}
Sum	—	824	0.4991×10^{-2}	875	0.8469×10^{-2}

* Number of selected modes

Furthermore, the failure probabilities P [$ZM_i \leq 0$]'s are calculated and given in Table 3, using the safety margins of the last hinged member ends in the final forms of structural failure shown in Fig. 4 (b). These safety margins are the same as those derived by applying the principle of virtual work as stated before. The failure probabilities of the minimum sets of failed member ends corresponding to the selected structural failure modes are larger than those corresponding to the discarded failure modes. This fact shows that the proposed method can automatically select the dominant failure modes needed for application of the conventional methods of reliability analysis and their safety margins.

Next, consider the relationship of the deterministically dominant modes of structural failure to the stochastically dominant modes. For the purpose, central load factors:

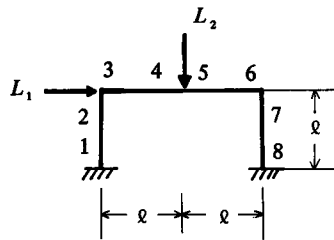
$$\lambda_i = \frac{\sum_{j=1}^n a_{ij} \bar{R}_j}{\sum_{j=1}^l b_{ij} \bar{L}_j} \quad (i = 1, 2, \dots, 13) \tag{25}$$

are calculated and listed in Table 3 for the final forms of structural failure shown in Fig. 4 (b). From the deterministic point of view, most dominant is the combined mechanism (xiii) which collapses to a mechanism under the minimum applied loads. On the contrary, the failure modes having the largest failure probabilities are the beam mechanisms (i) and (iv), which are not identical to the deterministically most dominant mode.

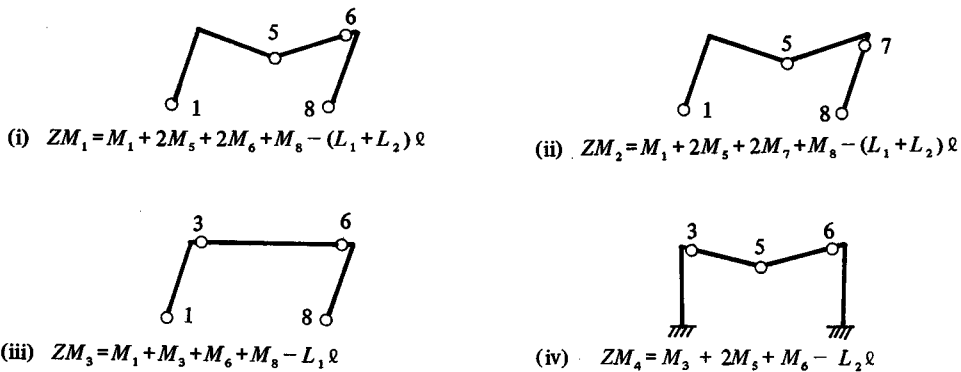
Finally, discussions are made of the calculated upper bounds. The upper bounds P_{fU} 's are smaller than the $P_{fU}^{(1)}$'s. However, they are fairly larger than $\sum_{i=1}^{13} P [ZM_i \leq 0]$ in Table 3. These discrepancies are seemed to be caused by the same reason as stated in the previous example.

4.3 Portal frame with combined loads

Reliability assessment is made of the portal frame with horizontal and vertical loads applied as shown in Fig. 6 (a). The data concerned are given in Table 1 and Fig. 6 (a), and the results are listed in Table 4 for various values of the correlation coefficients between the two loads. It is seen that the upper bound of the structural failure probability P_{fU} is considerably different depending on the value of the correlation coefficient. Consequently, it is very important to take into account of the correlation between the loads. Fig. 6(b)



(a) Portal frame with combined loads
 $(\bar{L}_1 = 50 \text{ kN}, \bar{L}_2 = 40 \text{ kN}, l = 5 \text{ m})$



(b) Dominant final forms of structural failure

Fig. 6 Portal frame with combined loads and dominant final forms of structural failure.

Table 4 Reliability assessment of portal frame with combined loads

Correlation coefficient $\rho_{L_1 L_2}$	Coefficients of variation ($CV_{\sigma Y_i} / CV_{L_j}$)				
	0.05 / 0.3	0.1 / 0.3	0.05 / 0.15	0.1 / 0.15	
1.0	P_{fU}	0.6958×10^{-1} (19)**	0.1202×10^0 (27)	0.2380×10^{-3} (8)	0.1298×10^{-2} (12)
	P_1^*	0.2871×10^{-1} (6)	0.3269×10^{-1} (6)	0.1142×10^{-3} (3)	0.4637×10^{-3} (6)
	P_2	0.6933×10^{-2} (4)	0.8944×10^{-2} (6)	0.1091×10^{-5} (3)	0.1591×10^{-4} (4)
	P_3	0.1703×10^{-2} (0)	0.2358×10^{-2} (2)	0.7947×10^{-8} (0)	0.2810×10^{-6} (0)
	P_4	0.4053×10^{-3} (4)	0.7878×10^{-3} (0)	0.1301×10^{-9} (0)	0.6794×10^{-7} (0)
	ΣP_i^{***}	0.3818×10^{-1}	0.4317×10^{-1}	0.1153×10^{-3}	0.4796×10^{-3}
	0.5	P_{fU}	0.6876×10^{-1} (29)	0.9132×10^{-1} (31)	0.7117×10^{-4} (11)
P_1		0.1904×10^{-1} (5)	0.2277×10^{-1} (7)	0.3175×10^{-4} (4)	0.2047×10^{-3} (5)
P_2		0.3635×10^{-2} (6)	0.5159×10^{-2} (6)	0.1449×10^{-6} (5)	0.4943×10^{-5} (5)
P_3		0.1703×10^{-2} (2)	0.2358×10^{-2} (2)	0.7947×10^{-8} (0)	0.2810×10^{-6} (1)
P_4		0.4053×10^{-3} (4)	0.7878×10^{-3} (5)	0.1301×10^{-9} (0)	0.6794×10^{-7} (0)
ΣP_i		0.2525×10^{-1}	0.3201×10^{-1}	0.3189×10^{-4}	0.2099×10^{-3}
0.0		P_{fU}	0.4212×10^{-1} (30)	0.6162×10^{-1} (35)	0.1316×10^{-4} (13)
	P_1	0.1055×10^{-1} (6)	0.1372×10^{-1} (6)	0.5156×10^{-5} (5)	0.7004×10^{-4} (5)
	P_2	0.1431×10^{-2} (5)	0.2392×10^{-2} (6)	0.8385×10^{-8} (5)	0.1097×10^{-5} (7)
	P_3	0.1703×10^{-2} (3)	0.2358×10^{-2} (3)	0.7947×10^{-8} (2)	0.2810×10^{-6} (2)
	P_4	0.4053×10^{-3} (5)	0.7878×10^{-3} (5)	0.1301×10^{-9} (0)	0.6794×10^{-7} (0)
	ΣP_i	0.1460×10^{-1}	0.1781×10^{-1}	0.5172×10^{-5}	0.7142×10^{-4}
	-0.5	P_{fU}	0.2256×10^{-1} (28)	0.3815×10^{-1} (37)	0.1277×10^{-5} (17)
P_1		0.4162×10^{-2} (5)	0.6372×10^{-2} (7)	0.3152×10^{-6} (6)	0.1607×10^{-4} (6)
P_2		0.3270×10^{-3} (4)	0.7528×10^{-3} (5)	0.1096×10^{-9} (7)	0.1459×10^{-6} (6)
P_3		0.1703×10^{-2} (3)	0.2358×10^{-2} (4)	0.7947×10^{-8} (2)	0.2810×10^{-6} (2)
P_4		0.4053×10^{-3} (6)	0.7878×10^{-3} (6)	0.1301×10^{-9} (0)	0.6794×10^{-7} (5)
ΣP_i		0.7102×10^{-2}	0.1118×10^{-1}	0.3233×10^{-6}	0.1657×10^{-4}
-1.0		P_{fU}	0.5651×10^{-2} (31)	0.2011×10^{-1} (41)	0.2707×10^{-7} (24)
	P_1	0.7485×10^{-3} (6)	0.1712×10^{-2} (4)	0.2405×10^{-8} (5)	0.1868×10^{-5} (7)
	P_2	0.2144×10^{-4} (2)	0.1066×10^{-3} (5)	0.6529×10^{-13} (2)	0.8475×10^{-8} (6)
	P_3	0.1703×10^{-2} (3)	0.2358×10^{-2} (4)	0.7947×10^{-8} (3)	0.2810×10^{-6} (4)
	P_4	0.4053×10^{-3} (6)	0.7878×10^{-3} (4)	0.1301×10^{-9} (5)	0.6794×10^{-7} (7)
	ΣP_i	0.3388×10^{-2}	0.5872×10^{-2}	0.1053×10^{-7}	0.2235×10^{-5}

Central load factor : $\lambda_1 = 1.50$, $\lambda_2 = 1.65$, $\lambda_3 = 1.89$, $\lambda_4 = 2.02$

* $P_i \triangleq P [ZM_i \leq 0]$: Failure probability of the mode based on conventional method.

** Figures in parentheses denote numbers of selected modes.

*** Sum of failure probabilities of all the possible final forms of structural failure.

illustrates the final forms of structural failure mode and their safety margins needed for application of the conventional methods. The central load factors and the failure probabilities of these safety margins are also listed in Table 4, which shows that the determinist-

ically, dominant mode is not always stochastically relevant and that the stochastically most dominant mode changes with the value of the correlation coefficient. Further, Table 4 includes for reference the numbers of the selected failure modes which are reduced to the same minimum sets of the failed member ends given in Fig. 6 (b). Failure probabilities corresponding to the other minimum sets are small compared to those listed in Table 4.

5. Concluding Remarks

This paper proposes the method for automatically generating failure modes of plane frame structures and mode equations by using a Matrix method and for estimating the upper bound of structural failure probability by systematically searching for the stochastically dominant modes of failure through branching and bounding operations. The properties of the proposed method are clarified by investigating the relationship between the proposed method and the conventional ones in which the failure modes need to be specified *a priori*. The proposed method is effective not only for reliability analysis of frame structures but also for determining the failure modes needed in the conventional methods. Further, the upper bound given by the proposed method is proved to be larger than the bound by the conventional methods where the relevant failure modes are predetermined. The numerical examples are provided to demonstrate the validity of the proposed method. Finally, it is suggested that a new method combining the proposed method with the conventional ones is most promising for reliability assessment of large-scale redundant frame structures, in which the present branching and bounding criteria need to be improved for the computation efficiency.

Acknowledgements

The authors would like to greatly appreciate the helps given by Mr. T. Toyama, Dr. R. Hosoda, and Dr. K. Tanaka who were the members of the special research group formed to accept the fourth author as a visiting research associate at the Department of Naval Architecture, University of Osaka Prefecture. The financial support of the joint research was partly provided by the Sonderforschungsbereich 96 of the Deutsche Forschungsgemeinschaft through dispatching the fourth author to the University of Osaka Prefecture. This work is also financially supported by the Scientific Research Fund of the Ministry of Education, Science and Culture of Japan. All the computations are processed by using ACOS/NEAC System 700 at the Computer Center of the University of Osaka Prefecture.

References

- 1) J. D. Stevenson and F. J. Moses, *J. Str. Div., Proc. ASCE*, **96** ST-11, 2409 (1972).
- 2) E. H. Vanmarcke, *Computers and Structures*, **3**, 757 (1973).
- 3) Y. Murotsu, *et al.*, *Proc. 12th International Symposium on Space Technology and Science*, Tokyo, 1047 (1977).
- 4) O. Ditlevsen, *J. Structural Mechanics*, **7**, 4, 435 (1979).
- 5) M. Yonezawa, *et al.*, *Trans. JSME*, **44**-385, 2936 (1978).
- 6) Y. Murotsu, *et al.*, (ed. by J. J. Burns), *Advances in Reliability and Stress Analysis*, p.3, ASME (1979).
- 7) M. Grimmelt, *Bull. Univ. Osaka Pref.*, **A**, **30**, 2, 41 (1981).
- 8) M. Shinozuka, *et al.*, *6th International Symposium on Space Technology and Science*, Tokyo, 431 (1965).
- 9) M. Shinozuka and H. Itagaki, *Annals of Reliability and Maintainability*, **5**, 605 (1966).
- 10) J. T. P. Yao and H-Y. Yeh, *J. Str. Div., Proc. ASCE*, **93**, ST-12, 2611 (1969).
- 11) Y. Murotsu, *et al.*, *Trans. ASME, J. Mech. Design*, **102**, 4, 749 (1980).
- 12) Y. Murotsu, *et al.*, *Trans. JSME*, **46**-404, A, 420 (1980).
- 13) Y. Murotsu, *et al.*, (ed. by M. D. Milestone), *Reliability, Stress Analysis and Failure Prevention in Mechanical Design*, p.81, ASME (1980).
- 14) Y. Murotsu, *et al.*, *Trans. JSME*, **47**-419, A, 763 (1981).
- 15) Y. Murotsu, *et al.*, (ed. by T. Moan and M. Shinozuka), *Structural Safety and Reliability*, p.315, Elsevier (1981).
- 16) V. B. Watwood, *J. Str. Div., Proc. ASCE*, **109**, ST-1, 1 (1979).
- 17) A. H. S. Ang and M. F. Ma; O. Klingmüller, (ed. by T. Moan and M. Shinozuka), *Structural Safety and Reliability*, p.295; p.331, Elsevier (1981).
- 18) Y. Yamamoto, *et al.*, *J. SNAJ*, **124**, 193 (1968).